Published in final edited form as:
Pharmacogenet Genomics. 2011 December ; 21(12): 798–807. doi:10.1097/FPC.0b013e32834b68f9.

Genes Linked to Energy Metabolism and Immunoregulatory Mechanisms are Associated with Subcutaneous Adipose Tissue Distribution in HIV-infected Men

Marguerite R Irvin[1], **Sadeep Shrestha**[1], **Yii-Der I. Chen**[2], **Howard W. Wiener**[1], **Talin Haritunians**[2], **Laura K. Vaughan**[3], **Hemant K. Tiwari**[3], **Kent D Taylor**[4], **Rebecca Scherzer**[5], **Michael S. Saag**[6], **Carl Grunfeld**[5], **Jerome I. Rotter**[2], and **Donna K. Arnett**[1]

[1]Department of Epidemiology, School of Public Health, University of Alabama at Birmingham

[2]Medical Genetics Institute, Cedars-Sinai Medical Center, University of Alabama at Birmingham

[3]Department of Biostatistics, School of Public Health, University of Alabama at Birmingham

[4]Pediatrics, School of Medicine, University of California Los Angeles

[5]Veterans Affairs Medical Center, School of Medicine, University of California, San Francisco

[6]Division of infectious Diseases, School of Medicine, University of Alabama at Birmingham

Abstract

Objective—Genetic studies may help explain abnormalities of fat distribution in HIV-infected patients treated with antiretroviral therapy (ARV).

Methods—Subcutaneous adipose tissue (SAT) volume measured by magnetic resonance imaging (MRI) in leg, lower trunk, upper trunk, and arm was examined in 192 HIV-infected Caucasian men, ARV-treated from the Fat Redistribution and Metabolic Change in HIV infection (FRAM) study. Single nucleotide polymorphisms (SNPs) were assayed using the Illumina HumanCNV370-quad beadchip. Multivariate and univariate genome wide association analyses of the four SAT depots were implemented in PLINK software adjusted for age and ARV duration. Functional annotation analysis (FAA) using Ingenuity Systems Pathway Analysis tool (IPA) was carried out for markers with $P<10^{-3}$ near known genes identified by multivariate analysis.

Results—Loci (rs10504906, rs13267998, rs921231) in or near the anion exchanger solute carrier family 26, member 7 isoform a (*SLC26A7*) were strongly associated with upper trunk and arm SAT ($9.8*10^{-7} \leq P < 7.8*10^{-6}$). Loci (rs193139, rs7523050, rs1761621) in and near a gene rich region including G-protein-signaling modulator 2 (*GPSM2*) and syntaxin binding protein 3 (*STXBP3)* were significantly associated with lower body SAT depots ($9.9*10^{-7} \leq P < 9.5*10^{-6}$). *GPSM2* is associated with cell division and cancer while *STXBP3* is associated with glucose metabolism in adipoctyes. IPA identified atherosclerosis, mitochondrial function and T-Cell mediated apoptosis as processes related to SAT volume in HIV-infected individuals ($P<5*10^{-3}$).

[*]**Corresponding Author** Marguerite R Irvin Department of Epidemiology University of Alabama at Birmingham, 1665 University Blvd, RPHB Room 220P Birmingham, Alabama 35294-0022 Phone: (205) 934 6459; Fax: (205) 934 8665 irvinr@uab.edu.

Conflicts of interest

The authors report there are no conflicts of interest to disclose

Conclusions—Our results are limited by the small sample size and replication is needed, however this genomic scan uncovered new genes associated with metabolism and inflammatory pathways that may affect SAT volume in ARV-treated HIV-infected patients.

Keywords

HIV; HAART; GWAS; Subcutaneous Fat; SAT

Introduction

The availability of combination ARV (also known as highly active antiretroviral therapy or HAART) in the mid 1990s has revolutionized HIV care by markedly improving survival and quality of life in patients [1;2]. Combination ARV does not, however, cure HIV infection, and those initiated on treatment will presumably be on ARV for life [3]. Extended use has been associated with both acute and chronic toxicities that limit ARV success [4], most notably changes in body shape [5]. The terms ‘fat redistribution syndrome’ and ‘lipodystrophy’ were initially used to describe a syndrome of fat loss in the periphery (lipoatrophy) accompanied by central fat gain (lipohypertrophy). The proposed syndrome has been associated with adverse cardiovascular outcomes, patient related stigma, and treatment non-compliance [6;7]. Early reports, however, were based on self-report focusing on questions that assessed local fat changes in a unidirectional manner, and did not include comparison to healthy controls [8;9].

Recent research targeting regional adipose tissue depots has challenged popular views of the syndrome itself [5;9;10]. The Fat Redistribution and Metabolic Change in HIV infection (FRAM) study characterized specific peripheral and central subcutaneous adipose tissue (SAT) depots by self-report and direct measurement using total body regional magnetic resonance imaging (MRI) in both HIV-infected individiuals and healthy controls. A major finding of the FRAM study was that HIV-infected participants differed from controls in terms of lipoatrophy, but not lipohypertrophy [8;10]. In HIV-infected men, legs and lower trunk SAT were more affected than upper trunk SAT, and lipoatrophy was self-reported to be mild in at least half the cases. Importantly, there was no reciprocal increase in central fat including visceral fat (VAT) [8]. Less leg SAT was associated with use of specific antiretroviral drugs, especially stavudine (d4T), but not any ARV class (including combination ARV) after accounting for specific drugs [8;10]. Other studies have noted the increased severity of lipoatrophy with d4T relative to other ARV drugs as well [11;12]. Similar studies of FRAM HIV+ women versus female controls were consistent, but outcomes were less severe [10]. For instance, FRAM investigators have shown that 49% of HIV+ men had leg SAT volume (measured by MRI) below the 10th percentile of healthy controls, compared with 32% of HIV+ women from FRAM, plus lipoatrophy was more severe in Caucasians than African Americans [13]. Since the degree of fat loss in HIV-infected patients treated with these medications is variable, it has been postulated that genetics may play a role in lipoatrophy accompanying exposure to ARV [14]. Plus, use of genetic studies may help advance our understanding of the etiology of adipose tissue changes. To date, there have been candidate gene studies focused on adipose tissue distribution in HIV-infected patients that have largely yielded inconsistent findings [14]. In the current study we conducted a genome wide association study (GWAS) of regional body SAT depots in a group of HIV-infected Caucasian men with a high prevalence of lipoatrophy from the FRAM study.

Methods

The FRAM study was initially designed to evaluate the prevalence and correlates of changes in fat distribution, insulin resistance, and dyslipidemia in a representative sample of HIV-infected participants and population-based controls in the United States [15].

Study Population

Between June 2000 and September 2002, FRAM enrolled 1,183 HIV-infected persons (70% male) from 16 participating HIV or infectious disease clinics and 297 controls from the Coronary Artery Risk Development in Young Adults (CARDIA) study. We recently conducted a GWAS including a small subset of the 1,183 participants. We identified 192 HIV-infected Caucasian men with historical and/or current use of d4T, and with measurements of common and internal carotid intima–media thicknesses (cIMT) [16]. The current study uses the genomic data collected for that study and MRI phenotypes collected for those participants at the baseline FRAM visit. Research associates interviewed participants and reviewed medical charts regarding ARV drug use. Consent was obtained from all FRAM participants and the protocol was approved by institutional review boards at all sites.

Adipose Tissue Measurement

Whole body MRI was performed to quantify regional and total adipose tissue, as described in detail elsewhere [8;17]. In brief, using the inter-vertebral space between the fourth and fifth lumbar vertebrae as origin, transverse images (10 mm slice thickness) were obtained every 40 mm from head to foot. MRI scans were segmented using image analysis software Slice-O-Matic (Tomovision Inc., Montreal, Canada). Imaging techniques and anatomical sites (based on bone landmarks) were identical between HIV-infected and control participants using a standardized and monitored acquisition protocol. All scans were sent to and read by investigators at the image reading center (IRC) located at the Obesity Research Center, St. Luke's Roosevelt Hospital, New York, NY. Tissue areas (cm^2) were calculated by summing specific tissue pixels, then multiplying by individual pixel surface area. Volume per slice (cm^3) of each tissue was calculated by multiplying area by thickness. Volume of each tissue for the space between two consecutive slices was calculated via a mathematical algorithm given in Shen et al. [18]. Anatomic sites considered in this analysis were: leg, lower trunk (abdomen and back), upper trunk (chest and back), and arm. The difference in results on repeated measurements as determined at the IRC was an average 1.1% for adipose tissue [17]. As in a previous analysis in FRAM, lipoatrophy was defined as leg subcutaneous adipose tissue volume below the cutoff marking the lowest decile (10%) of uninfected control men [13].

Genotyping methods and Quality Control (QC)

Genotyping methods have been previously described [16]. Briefly, blood samples were collected during the baseline visit and consent was obtained for storage of biological specimens for future use. Qiagen kits (Qiagen, Valencia, California, USA) were used to extract DNA. Genotyping was accomplished by use of the Illumina HumanCNV370-quad beadchip (Illumina, San Diego, CA, USA) housing 373,397 markers genotyped with the Infinium Assay. As part of our QC procedures, we flagged and removed the following from this report: individual non-monomorphic autosomal SNPs (N=333,737) with more than 3% missing data (N=8156), Hardy Weinberg equilibrium (HWE) $P<1*10^{-4}$ (N=767), and/or with low minor allele frequencies (MAF <1%, N=4996).

Statistical Analysis

Previous research in FRAM suggests HIV-infected men suffer from lipoatrophy at both peripheral and central fat depots, with lower body affected more than upper body. Since the pathophysiology of lipoatrophy is not completely understood and some regions are more affected than others, we considered each SAT depot both individually and jointly. Using PLINK software v1.07 (http://pngu.mgh.harvard.edu/purcell/plink/) we conducted a multivariate and univariate quantitative trait analysis of SAT volume measured by MRI at depots of interest (i.e., leg, lower trunk, upper trunk, and arm) [19]. We tested additive effects of each of 319,818 autosomal SNPs meeting the QC criteria described above. Each trait was log transformed to meet the assumption of normality of residuals for linear modeling, with the exception that arm SAT was transformed by its inverse. Each trait was adjusted for age plus duration of treatment of stavudine (d4T), zidovudine (AZT), and/or didanosine (DDI) in years (as treatment duration contributed to variation in the trait with $P<0.01$), since previous reports both in FRAM and other studies have found these treatments to be associated with SAT loss [20-22]. The presence of population substructure can be an important confounder in genetic association studies. We have previously reported this population to be very genetically homogeneous, and in the current study we considered our results with and without substructure adjustment using the first 3 principle components obtained with Eigenstrat software as previously described [16;23]. Adjustment for population substructure did not alter our conclusions and we report estimates unadjusted for population substructure. Finally, like other studies of SAT measured by MRI in FRAM we did not adjust to body mass index (BMI), as BMI is influenced by the phenomenon being studied: quantity of fat [8].

We performed the multivariate GWAS for additive SNP effects using the MQFAM command in PLINK on the residuals for all four SAT depots output from the models described above [24]. The method uses canonical correlation analysis (CCA) to measure the association between two sets of variables: the genetic marker (independent variable) and *k* traits (here the four sets of residuals are the dependent variables) [25]. Specifically, CCA extracts the linear combination of traits that explain the largest possible amount of the covariation between the marker and the traits. The correlation coefficient between each individual trait and the linear combination of traits with maximum correlation with the marker is output by MQFAM as the loading. For the univariate analysis, the additive effect of each SNP was regressed on each individual trait transformed and adjusted for covariates as described above. The average regional SAT volume by genotype was estimated from these models for SNPs with $P \leq 10^{-6}$. Deviations from the expected test statistic null distribution were assessed through quantile-quantile (Q-Q) plots. For all 4 SAT depots, the observed *P*-values did not greatly differ from the expected values over a wide range of values of $[-\text{Log}_{10}(P)]$ (Supplemental Figure 1). Linkage disequilibrium between SNPs of interest located in the same chromosomal region was calculated in Haploview version 4.1 [26]. The UCSC Genome Browser was used to locate genes near the most statistically significant markers considering a 200 kilobase (kb) window on either side of the marker [27]. The Gene Sorter program was then used to identify expression patterns, homology and other information about related genes [28].

The results of the multivariate analysis were used to conduct a functional annotation analysis (FAA) using the Ingenuity Pathway Analysis (IPA) tool (Ingenuity Systems, http://www.ingenuity.com). Genes (N=286) that were within a 50 kb window (to allow for inclusion of markers in 5' and/or 3' UTR regulatory regions) of SNPs from the multivariate GWAS analysis with $P<10^{-3}$ (corresponding to the top 396 SNPs) were selected for analysis in IPA (for a list of genes see Supplemental Table 1). The IPA Knowledge Base captures enrichment information from the Kyoto Encyclopedia of Genes and Genomes (KEGG), Gene Ontology (GO), Online Mendelian Inheritance in Man (OMIM), Entrez Gene, RefSeq

and others. Using its Knowledge Base, IPA identifies the most significant biological functions, diseases and canonical pathways associated with the gene list. A right-tailed Fisher's exact test is used to calculate an enrichment score *P*-value determining whether the association of each biological function and/or disease assigned to that data set is due to chance alone. In addition to obtaining enrichment scores from IPA we also employed the freely available Disease Association Protein-Protein Link Evaluator (DAPPLE; http://www.broadinstitute.org/mpg/dapple/dapple.php) to examine the physical connectivity among the gene list described above [29]. Using its knowledge base, InWeb, DAPPLE builds direct and indirect interaction networks from input genes and assesses their statistical significance [30].

Results

The mean age (±SD) of the 192 Caucasian men from FRAM at the baseline visit was 44.7±9 years. They had 1.9±2 years of exposure to d4T, 2.7±2 years of exposure to AZT and 0.8±1 years of exposure to DDI. Among the HIV-infected men included in this analysis 62% had peripheral lipoatrophy according to the definition of Kosmiski et al. [13]. The unadjusted average leg, lower trunk, upper trunk and arm SAT volume (L) measured by MRI was 2.8±1.0, 3.5±2.0, 2.9±1.0, and 1.1±0.4, respectively. Individual SAT depots were found to be positively and statistically significantly correlated ($0.46 \leq r \leq 0.77$, $P<0.0001$).

A Manhattan plot was generated to highlight genomic regions that may jointly influence multiple depots. Specifically, we plotted $-\text{Log}_{10}(P)$ from the multivariate association analysis against genome position by chromosome (Figure 1). Table 1 presents the most statistically significant results from the multivariate analysis ($P<10^{-6}$). Corresponding $-\text{Log}_{10}(P)$ for the markers presented in Table 1 are also enlarged in Figure 1. In Table 1, a larger loading for an individual trait reflects a larger contribution of that particular trait to the association result. No SNP was significantly associated with any trait with $P \leq 1.6*10^{-7}$ as would be required the conservative Bonferroni adjustment based on total number of markers tested.

Estimated SAT volume by genotype for SNPs with the strongest signals ($P<10^{-6}$) from the univariate GWAS analysis for each individual SAT depot is presented in Table 2. For all but one of the SNPs (rs1993976) presented in Table 2, the minor allele is associated with less SAT volume. This suggests that carrying the minor allele at these potential risk loci could be related to lipoatrophy in ARV treated HIV+ men. SNPs located on chromosome 1 p13.3 (rs193139 and rs7523050) and chromosome 8 q21.3 (rs921231) were amongst the most statistically significant markers identified in both the multivariate and univariate GWAS (Tables 1 and 2, respectively). Burgeoning support that these regions harbor loci associated with SAT distribution in HIV-infected patients, Figures 2a (chromosome 1) and 2b (chromosome 8) display other markers at least marginally associated ($P<10^{-4}$) with more than one SAT depot in the respective regions on chromosomes 1 (rs17621621) and 8 (rs10504906, rs13267998, rs7012492, rs10504908, rs16914136).

We used the Ingenuity Systems Pathway Analysis tool (IPA) to identify potential pathways, functions and diseases common to genes identified by our multivariate GWAS analysis. The top results from IPA are presented in Table 3. The FAA tool identified cardiovascular disease as the condition most significantly related to our gene list ($P<6.0*10^{-6}$). Specifically, 41 genes belonging to the original list of 286 were annotated for association with coronary artery disease and atherosclerosis. Genes related to cellular assembly and organization having to do with integrity of the mitochondria topped the cellular function annotation list ($P=1.2*10^{-3}$). Finally, cytotoxic T lymphocyte-mediated apoptosis of target cells was the top canonical pathway identified by IPA ($P=4.9*10^{-3}$). The results from DAPPLE showed 28

pair-wise, direct protein-protein interactions among our list of 286 genes (data not shown) and one gene, *HLA-DQA2*, was more connected than would be expected by chance to other proteins (CD3G and CD3D) on the input list (P=0.040) which is consistent with the canonical pathway highlighted by IPA in Table 3.

Discussion

In this GWAS of MRI-measured regional subcutaneous adipose tissue in HIV-infected, Caucasian men, we identified several novel loci near genes that may be implicated in both lipoatrophy associated with antiretroviral therapy and cardiovascular disease risk. To the best of our knowledge, this is the first genome-wide association study of MRI measured SAT in HIV-infected patients. There have been several candidate gene studies and gene expression studies seeking to identify risk factors for lipoatrophy, lipohypertrophy, or a combination of the two that focused on biologically plausible gene variants. Those studies included variants in mitochondrial DNA (mtDNA) and inflammatory markers (*TNF-α, IL-6, IL-1β*), or variants in genes related to adipocyte metabolism (*PPARγ, APOC3, ADRB2, ADRB3, RETN*, *LPIN1*, *CEBPA*) and apoptosis (*FAS*) [14;31-43]. The majority of results have been negative or inconclusive with the exception that the adiposity related genes adrenergic beta 2 receptor (*ADRB2)*, lipin 1 (*LIPIN1*), CCAAT/enhancer binding protein alpha (*CEBPA*) and resistin (*RETN)* genes have been implicated in combination ARV-related lipodystrophy [40;42;43]. Additionally, a study of HIV+ Caucasians from Spain (N=299) reported a coding SNP in *RETN* (-420C>G) was associated with ARV related lipodystrophy, at least marginally (P=0.04), and that patients with lipodystrophy had higher plasma resistin levels [44]. Our study did not replicate any previous specific gene findings, but uncovered new markers near genes related to inflammation, apoptosis, and metabolism.

The pattern of association of SNPs common to more than one fat depot may help focus on regions that are especially good candidates for being associated with ARV related lipoatrophy. Specifically, a previous FRAM report noted HIV-infected men had less SAT than controls, and that for these men the legs and lower trunk were more affected than upper trunk [8]. Interestingly, we found a group of markers (rs7523050, rs193139, rs1762161) on chromosome 1 spanning 100 kilobases (kb) for which the minor allele was associated with less SAT volume at each depot, but most significantly associated with lower body (leg and lower trunk) SAT. The three markers are tightly linked (two-way r^2>0.72) and lie in a gene rich area (Figure 2a). Though we were unable to identify any specific function of rs7523050, it is 5' to G-protein-signaling modulator 2 (*GPSM2*, chr1:109,221,126-109,274,567). *GPSM2* is an interesting candidate as it modulates activation of G proteins and has been linked to breast cancer cell division [45]. The marker rs193139 is intronic to chloride channel CLIC-like 1 (*CLCC1*, chr1:109,273,653-109,307,622) a widely expressed chloride channel located in the membranes of intracellular organelles [46]. The third marker, rs1762161, is intronic to AKNA domain containing 1 (*AKNAD1*, chr1:109160048-109201239) which is not yet well-characterized [28]. Another interesting nearby candidate gene (about 100 kb upstream) is syntaxin binding protein 3 (*STXBP3*, chr1:109,090,808-109,153,671) that may play a role in insulin-dependent movement of GLUT4 in adipocytes [47]. Future targeted studies of the region may clarify the risk gene and its functional variants that could be useful for predicting risk for lipoatrophy among HIV-infected individuals on ARV therapy.

The loci (rs502514) in the ubiquitination factor, *UBE4A*, is uniquely associated (P<$2.2*10^{-6}$) with leg SAT volume (Table 2). UBE4A (chr11:117,735,512-117,775,136) has been linked to multiple forms of cancer and is expressed in multiple cells of the immune system including T-cells, B-cells and lymphoctypes [28;48;49]. Nucleoside reverse transcriptase inhibitors (NRTIs) such as stavudine promote the ubiquitination and

downregulation of protein kinase C (PKC) an upstream regulator of peroxisome proliferator-activated receptor gamma (PPARγ) [50]. PPARγ is required for adipocyte differentiation [51]. To our knowledge there are no published data showing that *UBE4A* is expressed in adipose tissue. However, using total human adipose tissue RNA obtained from Clontech Laboratories (Mountain View, CA), our lab showed abundant *UBE4A* mRNA levels measured by real-time quantitative PCR (data not shown). Whether the peripheral lipoatrophy caused by d4T exposure is mediated by the ubiquitination factor *UBE4A* through the mechanism described above is a topic of future research.

Other regions seem to be more associated with upper body SAT. In our study a SNP (rs921231) in intron 8 of solute carrier family 26, member 7 isoform b (*SLC26A7,* chr8:92,330,692-92,476,122) is the top hit from the multivariate GWAS with $P=9.8*10^{-7}$(Table 1) and one of the top hits for upper trunk SAT (Table 2: $P=2.2*10^{-6}$). Additionally, two markers downstream from the gene (rs10504906, rs13267998) are strongly associated with arm SAT (Table 1 and Figure 2b). Each is in tight linkage disequilibrium (r^2 >0.80) with more than one marker in the 3' UTR of *SLC26A7*. *SLC26A7* is an ion exchanger and/or chloride transporter that is expressed in the basolateral membrane of acid-secreting cells in the kidney and stomach [52]. The gene has been associated with distal renal tubular acidosis and decreased gastric acid secretion in humans and mice [52]. The gastrointestinal tract participates in the regulation of energy homeostasis where gastrointestinal peptides participate in gastric acid release and signal to other tissues including adipose tissue through complex interactions [53]. Other markers associated with arm SAT (Table 2) were near genes linked to energy metabolism as well. These include rs1993976 which lies about 100 kb downstream of arrestin domain containing 4 (*ARRDC4,* chr15:96,304,937-96,318,072) that has been shown to inhibit glucose uptake in adipocytes in cell culture [54]. Additionally, rs10479469 was about 32 kb downstream of glutamine-fructose-6-phosphate transaminase 2 (*GFPT2,* chr5:179,660,306-179,712,921) that controls the flux of glucose in the hexosamine pathway and has been linked to insulin resistance [55].

Pathway-based approaches use prior biological knowledge to facilitate identification of related groups of genes associated with the phenotype that would otherwise be difficult to uncover due to small effect size and/or significance [56]. Our analysis using IPA revealed genes related to cardiovascular disease (CVD) were over-represented in our dataset (Table 3). This is biologically plausible as cardiovascular disease is another ARV-related side-effect that may be mediated through the same pathways [4]. IPA also highlighted genes with immunoregulatory function. Galectin-1 (*LGALS1)* and optic atrophy 1 (*OPA1*), a mitochondrial protein, were linked to mitochondrial fusion which is the most significant cellular function related to our data [57]. Mitochondria are dynamic organelles constantly fusing and dividing in response to different stimuli and metabolic demands. Instability of these processes can trigger apoptosis and disease [58] and, interestingly, other studies have suggested that mitochondrial dysfunction may contribute to HIV-associated lipoatrophy [14;59;60]. The top canonical pathway associated with our data was cytotoxic T-lymphocyte-mediated apoptosis of target cells. Genes related to this pathway included in our data were major histocompatibility complex, class II, DQ beta 2 (*HLA-DQB2*), major histocompatibility complex, class II, DQ alpha 2 (*HLA-DQA2*), and subunits of the T-cell receptor/CD3 complex (*CD3G* and *CD3D*) [28]. Additionally, DAPPLE highlighted this gene set as well. Specifically, *HLA-DQA2* was DAPPLE's top gene to prioritize based on connections with *CD3G* and *CD3D* [29]. In summary, a deeper mining of our data uncovered new targets for understanding how apoptotic pathways may contribute to lipoatrophy in HIV-infected patients.

Despite recent advances in understanding the morphologic changes in HIV-infected patients treated with ARV, the mechanisms underlying the processes are incompletely understood.

Genetic studies like ours can help to further define the etiology of lipoatrophy in HIV infection. Our study is cross-sectional in nature, did not include controls, and is of limited sample size. However, this subgroup (HIV+ Caucasian men exposed to d4T) with the highest risk for ARV related lipoatrophy, allowed us to reduce phenotype heterogeneity, an approach that has been suggested to reduce noise and enhance the likelihood of identifying novel risk loci [61]. The results of this study bolster support for the existence of genetic factors associated with this adverse treatment effect. We emphasize the results need to be replicated by expanding whole genome studies into the rest of FRAM (including healthy controls) and other cohorts to refine the genetic underpinnings of lipoatrophy in HIV that could vary by or be modified by gender, race and/or treatment. In conclusion, the current GWAS highlights many interesting genetic loci with plausible biological association to SAT. Markers in genes (or their regulatory regions) related to energy metabolism, cardiovascular disease and apoptosis are highlighted and suggest these pathways are important to the physiology of lipoatrophy in HIV-infected patients on ARV therapy.

Supplementary Material

Refer to Web version on PubMed Central for supplementary material.

Acknowledgments

We thank investigators and staff of the Fat Redistribution and Metabolic Change in HIV Infection (FRAM) study. The parent study and this sub-study conformed to the procedures for informed consent approved by institutional review boards at all sponsoring organizations and to human-experimentation guidelines set forth by the United States Department

Support: The FRAM study was supported by NIH grants RO1-DK57508, HL74814, and HL 53359, K23 AI66943, & UL1 RR024131; NIH GCRC grants M01- RR00036, RR00051, RR00052, RR00054, RR00083, RR0636, & RR00865; the Albert L. and Janet A. Schultz Supporting Foundation; and with resources and the use of facilities of the Veterans Affairs Medical Centers of, Atlanta, District of Columbia, New York and San Francisco. Clinicaltrials.gov ID: NCT0033144. Additional funding sources include K01 DK080188 and T32 NS054584.

Reference List

1. Gazzard B. Antiretroviral therapy for HIV: medical miracles do happen. Lancet. 2005; 366:346–347. [PubMed: 16054922]
2. Greenberg B, McCorkle R, Vlahov D, Selwyn PA. Palliative care for HIV disease in the era of highly active antiretroviral therapy. J Urban Health. 2000; 77:150–165. [PubMed: 10855997]
3. Finzi D, Blankson J, Siliciano JD, Margolick JB, Chadwick K, Pierson T, et al. Latent infection of CD4+ T cells provides a mechanism for lifelong persistence of HIV-1, even in patients on effective combination therapy. Nat Med. 1999; 5:512–517. [PubMed: 10229227]
4. Carr A, Cooper DA. Adverse effects of antiretroviral therapy. Lancet. 2000; 356:1423–1430. [PubMed: 11052597]
5. Khara M, Conway B. Morphologic changes in HIV-infected men: sorting fact from fiction. J Acquir Immune Defic Syndr. 2005; 40:119–120. [PubMed: 16186727]
6. Bevilacqua M, Dominguez LJ, Barbagallo M. Insulin Resistance and the cardiometabolic syndrome in HIV infection. J Cardiometab Syndr. 2009; 4:40–43. [PubMed: 19245515]
7. Duran S, Saves M, Spire B, Cailleton V, Sobel A, Carrieri P, et al. Failure to maintain long-term adherence to highly active antiretroviral therapy: the role of lipodystrophy. AIDS. 2001; 15:2441–2444. [PubMed: 11740195]
8. Bacchetti P, Gripshover B, Grunfeld C, Heymsfield S, McCreath H, Osmond D, et al. Fat distribution in men with HIV infection. J Acquir Immune Defic Syndr. 2005; 40:121–131. [PubMed: 16186728]
9. Tien PC, Grunfeld C. What is HIV-associated lipodystrophy? Defining fat distribution changes in HIV infection. Curr Opin Infect Dis. 2004; 17:27–32. [PubMed: 15090886]

10. Fat distribution in women with HIV infection. J Acquir Immune Defic Syndr. 2006; 42:562–571. [PubMed: 16837863]
11. Martinez E. Disorders of fat partitioning in treated HIV-infection. Best Pract Res Clin Endocrinol Metab. 2011; 25:415–427. [PubMed: 21663836]
12. Han SH, Zhou J, Saghayam S, Vanar S, Phanuphak N, Chen YM, et al. Prevalence of and risk factors for lipodystrophy among HIV-infected patients receiving combined antiretroviral treatment in the Asia-Pacific region: results from the TREAT Asia HIV Observational Database (TAHOD). Endocr J. 2011; 58:475–484. [PubMed: 21521929]
13. Kosmiski LA, Bacchetti P, Kotler DP, Heymsfield SB, Lewis CE, Shlipak MG, et al. Relationship of fat distribution with adipokines in human immunodeficiency virus infection. J Clin Endocrinol Metab. 2008; 93:216–224. [PubMed: 17940113]
14. Vidal F, Gutierrez F, Gutierrez M, Olona M, Sanchez V, Mateo G, et al. Pharmacogenetics of adverse effects due to antiretroviral drugs. AIDS Rev. 2010; 12:15–30. [PubMed: 20216907]
15. Tien PC, Benson C, Zolopa AR, Sidney S, Osmond D, Grunfeld C. The study of fat redistribution and metabolic change in HIV infection (FRAM): methods, design, and sample characteristics. Am J Epidemiol. 2006; 163:860–869. [PubMed: 16524955]
16. Shrestha S, Irvin MR, Taylor KD, Wiener HW, Pajewski NM, Haritunians T, et al. A genome-wide association study of carotid atherosclerosis in HIV-infected men. AIDS. 2010; 24:583–592. [PubMed: 20009918]
17. Gallagher D, Belmonte D, Deurenberg P, Wang Z, Krasnow N, Pi-Sunyer FX, et al. Organ-tissue mass measurement allows modeling of REE and metabolically active tissue mass. Am J Physiol. 1998; 275:E249–E258. [PubMed: 9688626]
18. Shen W, Wang Z, Tang H, Heshka S, Punyanitya M, Zhu S, et al. Volume estimates by imaging methods: model comparisons with visible woman as the reference. Obes Res. 2003; 11:217–225. [PubMed: 12582217]
19. Purcell S, Neale B, Todd-Brown K, Thomas L, Ferreira MA, Bender D, et al. PLINK: a tool set for whole-genome association and population-based linkage analyses. Am J Hum Genet. 2007; 81:559–575. [PubMed: 17701901]
20. Dube MP, Parker RA, Tebas P, Grinspoon SK, Zackin RA, Robbins GK, et al. Glucose metabolism, lipid, and body fat changes in antiretroviral-naive subjects randomized to nelfinavir or efavirenz plus dual nucleosides. AIDS. 2005; 19:1807–1818. [PubMed: 16227788]
21. Dube MP, Komarow L, Mulligan K, Grinspoon SK, Parker RA, Robbins GK, et al. Long-term body fat outcomes in antiretroviral-naive participants randomized to nelfinavir or efavirenz or both plus dual nucleosides. Dual X-ray absorptiometry results from A5005s, a substudy of Adult Clinical Trials Group 384. J Acquir Immune Defic Syndr. 2007; 45:508–514. [PubMed: 17589373]
22. Mulligan K, Parker RA, Komarow L, Grinspoon SK, Tebas P, Robbins GK, et al. Mixed patterns of changes in central and peripheral fat following initiation of antiretroviral therapy in a randomized trial. J Acquir Immune Defic Syndr. 2006; 41:590–597. [PubMed: 16652032]
23. Price AL, Patterson NJ, Plenge RM, Weinblatt ME, Shadick NA, Reich D. Principal components analysis corrects for stratification in genome-wide association studies. Nat Genet. 2006; 38:904–909. [PubMed: 16862161]
24. Ferreira MA, Purcell SM. A multivariate test of association. Bioinformatics. 2009; 25:132–133. [PubMed: 19019849]
25. Hotelling H. Relations between two sets of variables. Biometrika. 1936; 28:321–377.
26. Barrett JC, Fry B, Maller J, Daly MJ. Haploview: analysis and visualization of LD and haplotype maps. Bioinformatics. 2005; 21:263–265. [PubMed: 15297300]
27. Pevsner J. Analysis of genomic DNA with the UCSC genome browser. Methods Mol Biol. 2009; 537:277–301. [PubMed: 19378150]
28. Kent WJ, Hsu F, Karolchik D, Kuhn RM, Clawson H, Trumbower H, et al. Exploring relationships and mining data with the UCSC Gene Sorter. Genome Res. 2005; 15:737–741. [PubMed: 15867434]

29. Rossin EJ, Lage K, Raychaudhuri S, Xavier RJ, Tatar D, Benita Y, et al. Proteins encoded in genomic regions associated with immune-mediated disease physically interact and suggest underlying biology. PLoS Genet. 2011; 7:e1001273. [PubMed: 21249183]
30. Lage K, Hansen NT, Karlberg EO, Eklund AC, Roque FS, Donahoe PK, et al. A large-scale analysis of tissue-specific pathology and gene expression of human disease genes and complexes. Proc Natl Acad Sci U S A. 2008; 105:20870–20875. [PubMed: 19104045]
31. Martin AM, Hammond E, Nolan D, Pace C, Den Boer M, Taylor L, et al. Accumulation of mitochondrial DNA mutations in human immunodeficiency virus-infected patients treated with nucleoside-analogue reverse-transcriptase inhibitors. Am J Hum Genet. 2003; 72:549–560. [PubMed: 12587093]
32. Shikuma CM, Hu N, Milne C, Yost F, Waslien C, Shimizu S, et al. Mitochondrial DNA decrease in subcutaneous adipose tissue of HIV-infected individuals with peripheral lipoatrophy. AIDS. 2001; 15:1801–1809. [PubMed: 11579242]
33. Walker UA, Bickel M, Lutke Volksbeck SI, Ketelsen UP, Schofer H, Setzer B, et al. Evidence of nucleoside analogue reverse transcriptase inhibitor--associated genetic and structural defects of mitochondria in adipose tissue of HIV-infected patients. J Acquir Immune Defic Syndr. 2002; 29:117–121. [PubMed: 11832679]
34. Zaera MG, Miro O, Pedrol E, Soler A, Picon M, Cardellach F, et al. Mitochondrial involvement in antiretroviral therapy-related lipodystrophy. AIDS. 2001; 15:1643–1651. [PubMed: 11546938]
35. Maher B, Alfirevic A, Vilar FJ, Wilkins EG, Park BK, Pirmohamed M. TNF-alpha promoter region gene polymorphisms in HIV-positive patients with lipodystrophy. AIDS. 2002; 16:2013–2018. [PubMed: 12370499]
36. Nolan D, Moore C, Castley A, Sayer D, Mamotte C, John M, et al. Tumour necrosis factor-alpha gene -238G/A promoter polymorphism associated with a more rapid onset of lipodystrophy. AIDS. 2003; 17:121–123. [PubMed: 12478078]
37. Tarr PE, Taffe P, Bleiber G, Furrer H, Rotger M, Martinez R, et al. Modeling the influence of APOC3, APOE, and TNF polymorphisms on the risk of antiretroviral therapy-associated lipid disorders. J Infect Dis. 2005; 191:1419–1426. [PubMed: 15809899]
38. Asensi V, Rego C, Montes AH, Collazos J, Carton JA, Castro MG, et al. IL-1beta (+3954C/T) polymorphism could protect human immunodeficiency virus (HIV)-infected patients on highly active antiretroviral treatment (HAART) against lipodystrophic syndrome. Genet Med. 2008; 10:215–223. [PubMed: 18344712]
39. Saumoy M, Lopez-Dupla M, Veloso S, Alonso-Villaverde C, Domingo P, Broch M, et al. The IL-6 system in HIV-1-infection and in HAART-related fat redistribution syndromes. AIDS. 2008; 22:893–896. [PubMed: 18427208]
40. Ranade K, Geese WJ, Noor M, Flint O, Tebas P, Mulligan K, et al. Genetic analysis implicates resistin in HIV lipodystrophy. AIDS. 2008; 22:1561–1568. [PubMed: 18670214]
41. Saumoy M, Veloso S, Alonso-Villaverde C, Domingo P, Chacon MR, Miranda M, et al. PPARgamma Pro12Ala polymorphism in HIV-1-infected patients with HAART-related lipodystrophy. Curr HIV Res. 2009; 7:533–540. [PubMed: 19534662]
42. Zanone PB, Riva A, Nasi M, Cicconi P, Broggini V, Lepri AC, et al. Genetic polymorphisms differently influencing the emergence of atrophy and fat accumulation in HIV-related lipodystrophy. AIDS. 2008; 22:1769–1778. [PubMed: 18753860]
43. Pushpakom SP, Owen A, Vilar FJ, Castro H, Dunn DT, Back DJ, et al. Adipogenic gene variants in patients with HIV-associated lipodystrophy. Pharmacogenet Genomics. 2011; 21:76–83. [PubMed: 21178827]
44. Escote X, Miranda M, Veloso S, Domingo P, Alonso-Villaverde C, Peraire J, et al. Lipodystrophy and insulin resistance in combination antiretroviral treated HIV-1-infected patients: implication of resistin. J Acquir Immune Defic Syndr. 2011
45. Fukukawa C, Ueda K, Nishidate T, Katagiri T, Nakamura Y. Critical roles of LGN/GPSM2 phosphorylation by PBK/TOPK in cell division of breast cancer cells. Genes Chromosomes Cancer. 2010; 49:861–872. [PubMed: 20589935]

46. Nagasawa M, Kanzaki M, Iino Y, Morishita Y, Kojima I. Identification of a novel chloride channel expressed in the endoplasmic reticulum, golgi apparatus, and nucleus. J Biol Chem. 2001; 276:20413–20418. [PubMed: 11279057]
47. Spurlin BA, Park SY, Nevins AK, Kim JK, Thurmond DC. Syntaxin 4 transgenic mice exhibit enhanced insulin-mediated glucose uptake in skeletal muscle. Diabetes. 2004; 53:2223–2231. [PubMed: 15331531]
48. Contino G, Amati F, Pucci S, Pontieri E, Pichiorri F, Novelli A, et al. Expression analysis of the gene encoding for the U-box-type ubiquitin ligase UBE4A in human tissues. Gene. 2004; 328:69–74. [PubMed: 15019985]
49. Vazquez-Ortiz G, Garcia JA, Ciudad CJ, Noe V, Penuelas S, Lopez-Romero R, et al. Differentially expressed genes between high-risk human papillomavirus types in human cervical cancer cells. Int J Gynecol Cancer. 2007; 17:484–491. [PubMed: 17309674]
50. Bradshaw EL, Li XA, Guerin T, Everson WV, Wilson ME, Bruce-Keller AJ, et al. Nucleoside reverse transcriptase inhibitors prevent HIV protease inhibitor-induced atherosclerosis by ubiquitination and degradation of protein kinase C. Am J Physiol Cell Physiol. 2006; 291:C1271–C1278. [PubMed: 16822947]
51. Kawai M, Sousa KM, MacDougald OA, Rosen CJ. The many facets of PPARgamma: novel insights for the skeleton. Am J Physiol Endocrinol Metab. 2010; 299:E3–E9. [PubMed: 20407009]
52. Xu J, Song P, Nakamura S, Miller M, Barone S, Alper SL, et al. Deletion of the chloride transporter slc26a7 causes distal renal tubular acidosis and impairs gastric acid secretion. J Biol Chem. 2009; 284:29470–29479. [PubMed: 19723628]
53. Majumdar ID, Weber HC. Gastrointestinal regulatory peptides and their effects on fat tissue. Curr Opin Endocrinol Diabetes Obes. 2010; 17:51–56. [PubMed: 19855273]
54. Patwari P, Chutkow WA, Cummings K, Verstraeten VL, Lammerding J, Schreiter ER, et al. Thioredoxin-independent regulation of metabolism by the alpha-arrestin proteins. J Biol Chem. 2009; 284:24996–25003. [PubMed: 19605364]
55. Kaneto H, Xu G, Song KH, Suzuma K, Bonner-Weir S, Sharma A, et al. Activation of the hexosamine pathway leads to deterioration of pancreatic beta-cell function through the induction of oxidative stress. J Biol Chem. 2001; 276:31099–31104. [PubMed: 11390407]
56. Wang K, Li M, Hakonarson H. Analysing biological pathways in genome-wide association studies. Nat Rev Genet. 2010; 11:843–854. [PubMed: 21085203]
57. Dhirapong A, Lleo A, Leung P, Gershwin ME, Liu FT. The immunological potential of galectin-1 and -3. Autoimmun Rev. 2009; 8:360–363. [PubMed: 19064001]
58. Karbowski M. Mitochondria on guard: role of mitochondrial fusion and fission in the regulation of apoptosis. Adv Exp Med Biol. 2010; 687:131–142. [PubMed: 20919642]
59. Nolan D, Hammond E, Martin A, Taylor L, Herrmann S, McKinnon E, et al. Mitochondrial DNA depletion and morphologic changes in adipocytes associated with nucleoside reverse transcriptase inhibitor therapy. AIDS. 2003; 17:1329–1338. [PubMed: 12799554]
60. Garrabou G, Lopez S, Moren C, Martinez E, Fontdevila J, Cardellach F, et al. Mitochondrial damage in adipose tissue of untreated HIV-infected patients. AIDS. 2011; 25:165–170. [PubMed: 21150553]
61. Manolio TA, Collins FS, Cox NJ, Goldstein DB, Hindorff LA, Hunter DJ, et al. Finding the missing heritability of complex diseases. Nature. 2009; 461:747–753. [PubMed: 19812666]

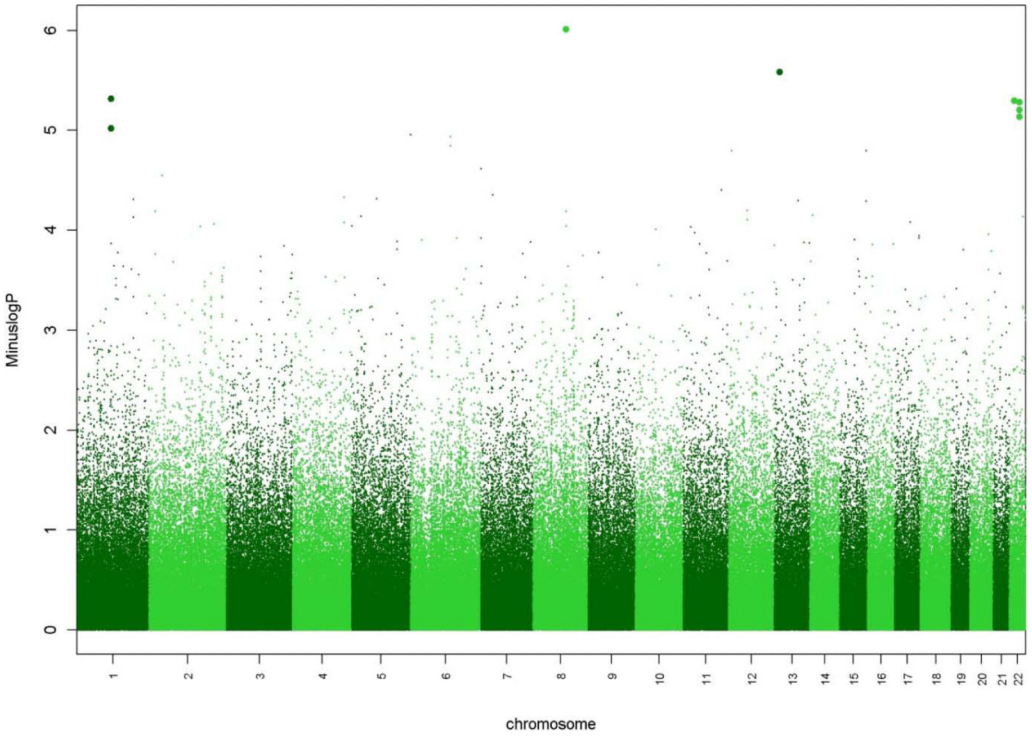

Figure 1.
Manhattan plot showing the genome wide association of single nucleotide polymorphisms (SNPs) with subcutaneous adipose tissue volume measured by MRI from the multivariate analysis. Statistical significance of SNPs is shown in the $-\log_{10}(P)$ scale. Values of $-\log_{10}(P)$ above 5 (i.e., results with strongest statistical significance) are enlarged and the corresponding markers are described in Table 1.

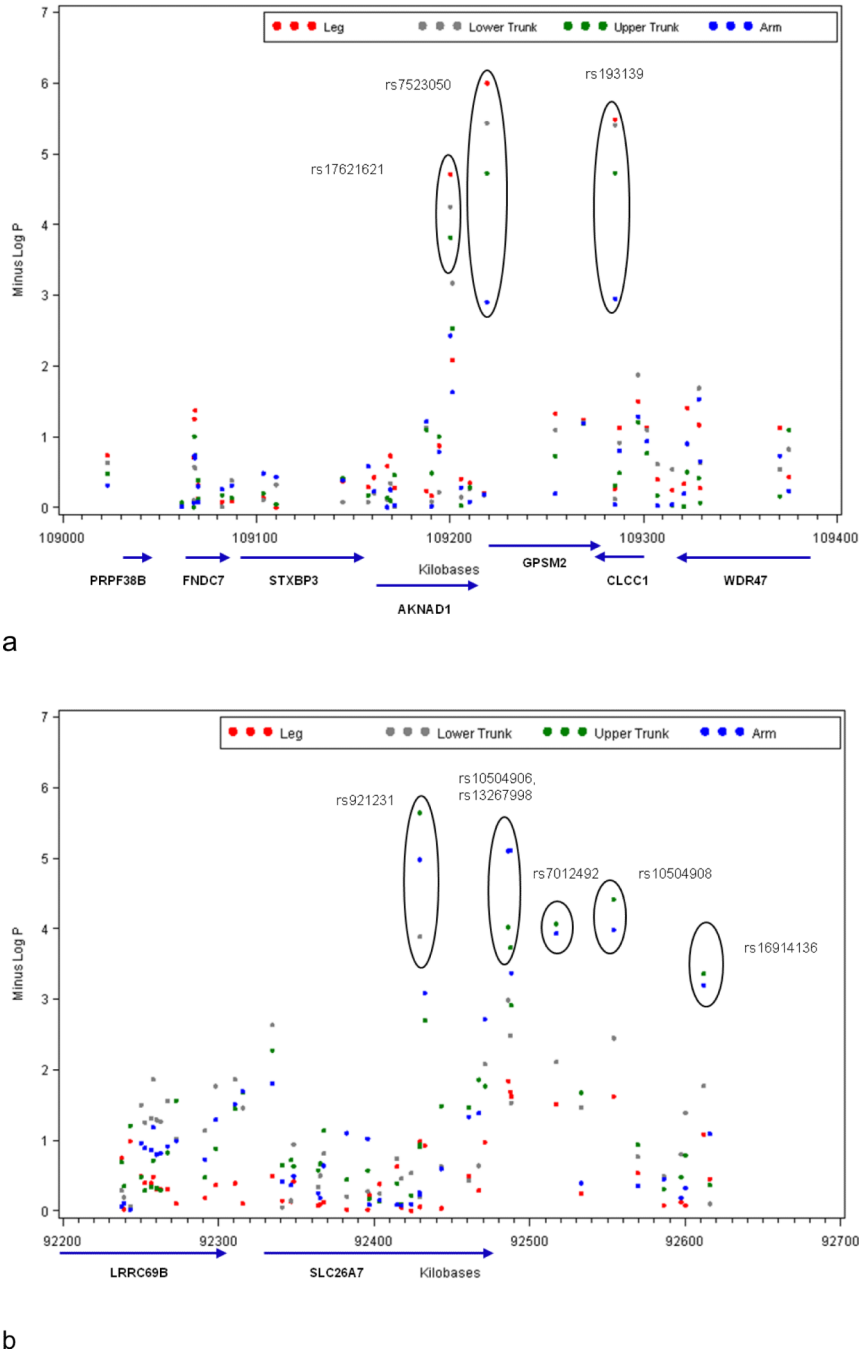

Figure 2.

a) Chromosome 1 regional association plot showing single nucleotide polymorphisms (SNPs) association with subcutaneous adipose tissue (SAT) volumes measured by MRI from the univariate genome wide analysis of each SAT depot. Results for leg, lower trunk, upper trunk and arm SAT are superimposed. Statistical significance of SNPs is shown in the -$\log_{10}(P)$ scale. b.) Same as 2a for chromosome 8.

Table 1

Top multivariate association results for subcutaneous adipose tissue volume (leg, lower trunk [LT], upper trunk [UT] and arm jointly considered as the outcome)

SNP	Coded (Major)	MAF	Chr	Position (BP)	Nearest Gene	Location	Loadings[#] Leg, LT, UT, Arm	*P*-Value
rs921231	G(A)	0.17	8	92429572	*SLC26A7*	Intronic	-0.3,-0.7,-0.8,0.8	$9.8^{*}10^{-7}$
rs7335631	C(A)	0.09	13	29855688	*KATNAL1*	-	0.3,0.1,0.5,0.1	$2.6^{*}10^{-6}$
rs7523050	A(C)	0.14	1	109219202	*GPSM2*	5’	-0.9,-0.8,-0.8,0.6	$4.8^{*}10^{-6}$
rs4417	A(G)	0.12	22	25746825	*MIAT*		0.5,0,-0.4,0.3	$5.0^{*}10^{-6}$
rs4820294	A(G)	0.35	22	36400989	*LGALS1*	-	-0.1,-0.5,-0.1,0.5	$5.2^{*}10^{-6}$
rs713835	A(G)	0.35	22	36394596	*PDXP*	-	-0.1,-0.5,-0.1,0.5	$6.2^{*}10^{-6}$
rs929039	G(A)	0.35	22	36401457	*LGALS1*	-	-0.1,-0.5,-0.1,0.5	$7.3^{*}10^{-6}$
rs193139	G(A)	0.14	1	109285498	*CLCC1*	Intronic	-0.9,-0.9,-0.8,0.6	$9.5^{*}10^{-6}$

[*] Single Nucleotide polymorphism (SNP), minor allele frequency (MAF), chromosome (Chr), base pair (BP)

[#] The loading is a correlation coefficient and reflects the contribution of that trait to the multivariate association results for that marker

Table 2

Top univariate association results for subcutaneous adipose tissue volume (leg, lower trunk, upper trunk and arm each considered individually as the outcome)

SNP*	Coded (Major)	MAF	Chr	Position (BP)	Nearest Gene	Location	SAT Volume (L) by Genotype#	*P*-Value
Leg^								
rs7523050	A(C)	0.14	1	109219202	*GPSM2*	5'	2.74 (1.8,4.2)	$9.9^{*}10^{-7}$
							2.04 (1.3,3.3)	
							1.52 (0.9,2.6)	
rs502514	G(A)	0.30	11	117747205	*UBE4A*	Intronic	2.88 (1.9,4.4)	$2.2^{*}10^{-6}$
							2.33 (1.5,3.7)	
							1.88 (1.2,3.1)	
rs193139	G(A)	0.14	1	109285498	*CLCC1*	Intronic	2.73 (1.8,4.1)	$3.2^{*}10^{-6}$
							2.08 (1.3,3.3)	
							1.59 (0.9,2.7)	
rs2342371	G(A)	0.28	3	197672005	*RNF168*	-	2.82 (1.9,4.3)	$4.4^{*}10^{-6}$
							2.31 (1.5,3.6)	
							1.88 (1.2,3.0)	
Lower Trunk (LT)^								
rs7523050	A(C)	0.14	1	109219202	*GPSM2*	5'	3.28 (1.7,6.2)	$3.7^{*}10^{-6}$
							2.18 (1.1,4.4)	
							1.45 (0.7,3.2)	
rs193139	G(A)	0.14	1	109285498	*CLCC1*	Intronic	3.28 (1.8,6.1)	$3.9^{*}10^{-6}$
							2.24 (1.1,4.4)	
							1.52 (0.7,3.3)	
rs7512221	G(A)	0.04	1	218668246	*MARK1*	-	3.11 (1.5,6.5)	$6.6^{*}10^{-6}$
							1.62 (0.7,3.9)	
Upper Trunk (UT)^								
rs13241427	C(A)	0.22	7	1255165	*UNCX*	-	2.91 (1.8,4.8)	$3.5^{*}10^{-7}$

SNP*	Coded (Major)	MAF	Chr	Position (BP)	Nearest Gene	Location	SAT Volume (L) by Genotype#	*P*-Value
							2.18 (1.3,3.7)	
							1.63 (0.9,2.9)	
rs13242133	G(A)	0.20	7	1255805	*UNCX*	-	2.89 (1.7,4.8)	$1.8^{*}10^{-6}$
							2.19 (1.3,3.8)	
							1.67 (0.9,3.0)	
rs921231	G(A)	0.17	8	92429572	*SLC26A7*	Intronic	2.80 (1.8,4.5)	$2.2^{*}10^{-6}$
							2.14 (1.3,3.5)	
							1.63 (0.9,2.9)	
rs1944766	C(A)	0.44	9	18205280	*ADAMTSL1*	-	3.10 (1.9,5.0)	$2.9^{*}10^{-6}$
							2.51 (1.5,4.2)	
							2.04 (1.2,3.5)	
***Arm*†**								
rs1993976	A(G)	0.39	15	96423836	*ARRDC4*	-	0.84 (0.6,1.2)	$8.2^{*}10^{-7}$
							0.98 (0.7,1.6)	
							1.19 (0.8,2.3)	
rs10479469	G(A)	0.33	5	179745274	*GFPT2*	-	1.05 (0.8,1.6)	$2.4^{*}10^{-6}$
							0.89 (0.7,1.3)	
							0.77 (0.6,1.1)	
rs10078	C(A)	0.23	5	491102	*AHRR*	3’ UTR	1.02 (0.7,1.6)	$7.4^{*}10^{-6}$
							0.85 (0.6,1.3)	
							0.73 (0.6,1.1)	
rs10504906	A(G)	0.07	8	92487804	*SLC26A7*	-	0.98 (0.7,1.5)	$7.5^{*}10^{-6}$
							0.76 (0.6,1.1)	
							0.63 (0.5,0.9)	
rs13267998	G(A)	0.07	8	92486443	*SLC26A7*	-	0.98 (0.7,1.5)	$7.8^{*}10^{-6}$
							0.77 (0.6,1.1)	
							0.64 (0.5,0.9)	

*Single Nucleotide polymorphism (SNP), minor allele frequency (MAF), chromosome (Chr), base pair (BP)

[#] in the order of major allele homozygote, heterozygote and minor allele heterozygote

[^] Outcome is ln(leg) adjusted for age and stavudine (d4T) duration; ln(LT) adjusted for age, d4T, zidovudine (AZT), and didanosine (DDI) duration; ln(UT) adjusted for age

[†] Outcome is 1/arm adjusted for age

Table 3

Top Pathways identified in Functional Annotation Analysis using Ingenuity Systems Pathway Analysis Tool (IPA)

Category	Function	Annotation	Molecules*	*enrichment P*-Value
1. Diseases and Disorders	Cardiovascular Disease	Coronary Artery Disease and Atherosclerosis	*A2BP1, ADAM12, ANKS1B, COL24A1, CSMD3, CTNNA2, CTNND2, DGKB, DIP2A, DSCAM, EYA4, F10, GRID2, GRM8, GUCY1A2, IGF2R, KIAA1199, LAMA4, MCF2L, MCM8, MEGF11, MON2, MTHFS, MYO10, NAALADL2, NBEA, NTN1, PARK2, PNPLA1, PPM1H, PPP1R9A, PSD3, PTPRM, RAB22A, RNF150, SLC26A7, SORCS2, THADA, TNIP3, TRPM3, WWOX*	$5.9^{*}10^{-6}$
2. Molecular and Cellular Functions	Cellular Assembly and Organization	Fusion of Mitochondria	*LGALS1, OPA1*	$1.2^{*}10^{-3}$
3. Canonical Pathway	Cytotoxic T Lymphocyte-mediated Apoptosis		*CD3G,HLA-DQB2,HLA-DQA2,CD3D*	$4.9^{*}10^{-3}$

*Human gene symbols approved by the HUGO Nomenclature Committee